J Mol Model (2010) 16:1187–1194
DOI 10.1007/s00894-009-0617-8

ORIGINAL PAPER

The theoretical and experimental study on dicalcium phosphate dehydrate loading with protocatechuic aldehyde

Yuehua Guo · Shuxin Qu · Xiong Lu · Haodong Xie · Hongping Zhang · Jie Weng

Received: 18 May 2009 / Accepted: 20 October 2009 / Published online: 18 December 2009
© Springer-Verlag 2009

Abstract The aim of this study is to investigate the interaction between dicalcium phosphate dihydrate ($CaHPO_4$•$2H_2O$, DCPD) and Protocatechuic aldehyde ($C_7H_6O_3$, Pca), which is the water-soluble constituents of Chinese Medicine, Salvia Miltiorrhiza Bunge (SMB), by calculating the absorption energy through molecular dynamics simulation. Furthermore, the effects of functional groups of Pca and temperature on Pca adsorbed by DCPD are calculated respectively. DCPD/Pca and DCPD were analyzed by X-ray diffraction (XRD), Fourier transform infrared spectroscopy (FTIR) and thermogravimetric analysis (TG). The simulation results showed that Pca mostly absorbed on the (0 2 0) surface of DCPD. The aldehyde group of Pca played a moren important role on the adsorption of Pca on DCPD than hydroxyl did, while temperature had no distinct effects on the adsorption. XRD results indicated that Pca induced the preferential growth of (0 2 0) crystal surface in DCPC/Pca whereas it had no influence on the crystal structure, the crystallinity and grain size of DCPD. FTIR and TG results showed that the characteristic peak of Pca was at 1295 cm^{-1} and the content of Pca in DCPD was 16%, respectively. The present results show that molecular dynamics simulation is a very effective and complementary method to study the interaction between materials and medicine.

Keywords Adsorption energy · Dicalcium phosphate dehydrate · Molecular dynamics · Protocatechuic aldehyde

Y. Guo · S. Qu (✉) · X. Lu · H. Xie · H. Zhang · J. Weng
Key Laboratory of Advanced Technologies of Materials, Ministry of Education, School of Materials Science and Engineering, Southwest Jiaotong University, Chengdu 610031, China
e-mail: qushuxin@swjtu.edu.cn

Introduction

Calcium phosphate cements (CPCs) were developed by Brown and Chow in the 1980s [1]. Since then, CPCs have been widely investigated as bone grafts due to their highly biocompatibility with tissues, biodegradability, contours adaptability and self-setting capability under ambient conditions with little heat release [2–4]. These properties have prompted intensive investigation of CPCs as the skeletal locally administrating therapeutic agents, such as various drugs and growth factors [3, 4].

Dicalcium phosphate dihydrate ($CaHPO_4·2H_2O$, DCPD) is one of the main components or the end-products of some CPCs [2]. DCPD has been detected in fracture callus, bone and other pathological calcification [2, 5]. It is also considered as the precursor of hydroxyapatite (HA) in bone, which DCPD is converted into (HA) [6] or biodegraded and replaced by bone in vivo [7]. Metastable DCPD can be converted into Dicalcium phosphate (DCPA, pH<6), Octocalcium phosphate (OCP, pH≈6–7) or Precipitated hydroxyapatite (PHA, pH>7) in vitro [2]. Thus DCPD is biocompatible, biodegradable and osteoconductive [2], which is one of the most important calcium phosphate salts.

Traditional Chinese medicines have been used in the Chinese population to treat bone diseases and to promote bone healing for thousands of years [8]. Among them, Salvia Miltiorrhiza Bunge (SMB) is a well-known Chinese medicine herb under the traditional Chinese name Dan-shen [9]. The major constituents of SMB are lipophilic compounds like a number of tanshinones and hydrophilics compounds like the protocatechuic aldehyde (Pca) or salvianolic acide B (SalB) [9]. Some researchers reported that SMB could accelerate the process of revascularization and re-ossification of bone healing in vivo [10] and

stimulate ALPase activity of osteoblasts in vitro although its leading application was in cardiovascular medicine [11]. Our previous study demonstrated that Pca presented the dose-dependent effects on the total metabolic activity of bone marrow cells [12].

Recently, some studies focused on the CaP based biomaterials loading Chinese medicine [13–16]. Lin et al. has reported that the Gusuibu, one Chinese medicine, can be immobilized chemically onto the surface-modified bioceramic calcium hydrogenphosphate ($CaHPO_4$, DCPA) and serve as an osteoinductive stimuli for bone graft [14]. It is found that the size of the osteoclasts is likely to decrease and the cell integrity seemed lost, while the osteoblasts phenotype expression is relatively preserved after treatment of Gusuibu-immobilized modified DCPA [15]. Yao et al. has prepared a novel biodegradable composite, composed of genipin crosslinked gelatin, tricalciun phosphate and traditional Chinese medicine. It is demonstrated that the composite can promote a significantly greater amount of bone regeneration with the presence of Chinese medicine [16]. In our previous study, calcium phosphate powder and cement loading SMB have been prepared and characterized [13, 17]. The release and degradation of calcium phosphate powder loading SMB has been investigated [18]. These studies of combining traditional Chinese medicine and biomedical materials are the increasing research field. However, how Chinese medicine interacts with biomaterials is still unclear, which would play an important role to determine the release of Chinese medicine. It is difficult to identify how Chinese medicine would interact with biomaterials due to their complex and indistinct ingredients and the limited analysis methodology.

Molecular dynamics (MD) is an important computer simulation method, which can be used to simulate the interaction between adsorbate and adsorbent at molecular and the nanometer scale [19]. Recently, molecular dynamics method was widely used. For example, density function theory (DFT) and MD methods have been employed to study the cyclopropane adsorption onto Cu (111) surfaces [19]. Based on the atomistic strength analyses of a type-I collagen and hydroxyapatite (HA) interfacial arrangement, Dubey et al. studied calcium phosphate materials to obtain the bone tissue fracture properties according to molecular dynamics [20]. Zhou et al. studied the adsorption mechanism of BMP-7 (one of the bone morphogenetic proteins, BMPs) on hydroxyapatite (001) surfaces [21] using molecular dynamics. Shen et al. studied protein adsorption and desorption on hydroxyapatite surfaces [22]. Bhowmik et al. also used molecular dynamics to simulate the hydroxyapatite-epolyacrylic acid interfaces [23]. MD simulations have often been used to evaluate interfacial behavior in composite systems [24].

Fig. 1 A DCPD unit cell

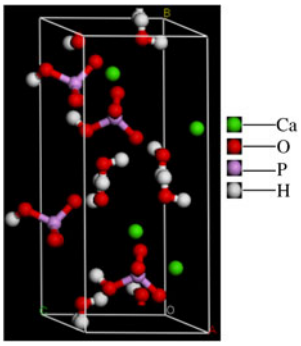

In our present study, MD was used to simulate theoretically the interaction between the effective ingredient of SMB, Protocatechuic aldehyde ($C_7H_6O_3$, Pca), and DCPD. Then Pca/DCPD was synthesized *via* the wet chemical methods and characterized by X-ray diffraction (XRD), thermogravimetric analysis (TG) and Fourier transform infrared spectroscopy (FTIR) to validate the theoretically results with experiments. The aim of the present study was to get a deeper understanding of the interaction between Pca and DCPD.

Experimental procedure

Simulation methods

DCPD and Pca structures

The simulations were performed with the Materials Studio (MS) v4.1 packages (Accelrys, San Diego, CA) using the condensed-phase optimized molecular potentials for atomistic simulation studies (COMPASS) force field [25]. DCPD as the mineral brushite has the monoclinic space group Ia with unit cell parameters a= 5.812 Å, b=15.180 Å, c=6.239 Å and β=116°25′ [26, 27]. The 3D structure of a DCPD crystal unit cell was shown in Fig. 1. Protocatechuic aldehyde is also called 3, 4-dihydroxybenzaldehyde [12]; and its structure was shown in Fig. 2.

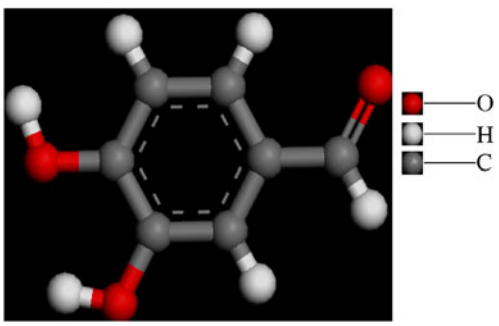

Fig. 2 A Pca molecule

Table 1 Lattice parameters of different DCPD crystal surfaces

Crystal surface	Depth	Lattice parameters (Å)		
		a	b	c
(0 2 0)	1.0	12.4780	11.6240	40.4654
(0 2 1)	2.0	18.8616	11.6240	34.6726
(0 4 1)	3.0	27.5447	11.6240	35.2296
(−2 2 1)	3.0	22.3900	16.2546	33.7491
(0 6 1)	3.0	36.8563	11.6240	33.5393
(−1 5 1)	3.0	12.7481	29.7086	33.1219

Molecular dynamics calculation

Six crystallographic planes of DCPD were selected: (0 2 0), (0 2 1), (0 4 1), (−2 2 1), (0 6 1) and (−1 5 1) [28]. The lattice parameters of these crystal surfaces are shown in Table 1. The Pca and H2O system was constructed through amorphous cell module. Then the system was added onto the as-built DCPD surface with 3D periodic boundary conditions to study the interaction between Pca and different DCPD surfaces. MD simulations were conducted under the canonical (NVT) ensemble at 298.0 K for 15 ps until the system reached equilibrium, and then additional 10 ps MD simulations were conducted for analysis, and the controlling method was Andersen [24, 29]. After calculation, the optimized structures of the systems were obtained and shown in Fig. 3.

The calculation of adsorption energy

A proper understanding of the mechanism in an adsorption process requires the accurate atom and structural information of the interactions between adsorbate and adsorbent as well for the reliable dynamic details of the whole adsorption processes [19]. The adsorption energy representing the degree of interaction between adsorbate and adsorbent during adsorption processes was derived according to Eq. 1 [19]:

$$E_{absorption} = E_{total} - E_{DCPD} - E_{Pca} - E_{H_2O} \quad (1)$$

Where E_{DCPD}, E_{H2O}, E_{Pca} and E_{total} represent the total energy of DCPD surface, the total energy of H_2O, the energy of the Pca without the DCPD surface and the adsorbed system (DCPD+Pca+H_2O), respectively. The influence of different temperature and functional groups on adsorption energy has been investigated.

Experimental method

Sample preparation

The analytical grade tetrahydrate calcium nitrate [$Ca(NO_3)_2{\cdot}4H_2O$] and diammonium phosphate [$(NH_4)_2HPO_4$] were used as starting materials to synthesize DCPD at the Ca: P molar ratio of 1.0 in our laboratory [13]. In brief, $(NH_4)_2HPO_4$ solution was dropped into the stirred Ca $(NO_3)_2$ solution accompanying the chemistry reference substance of Pca, which was purchased from the National

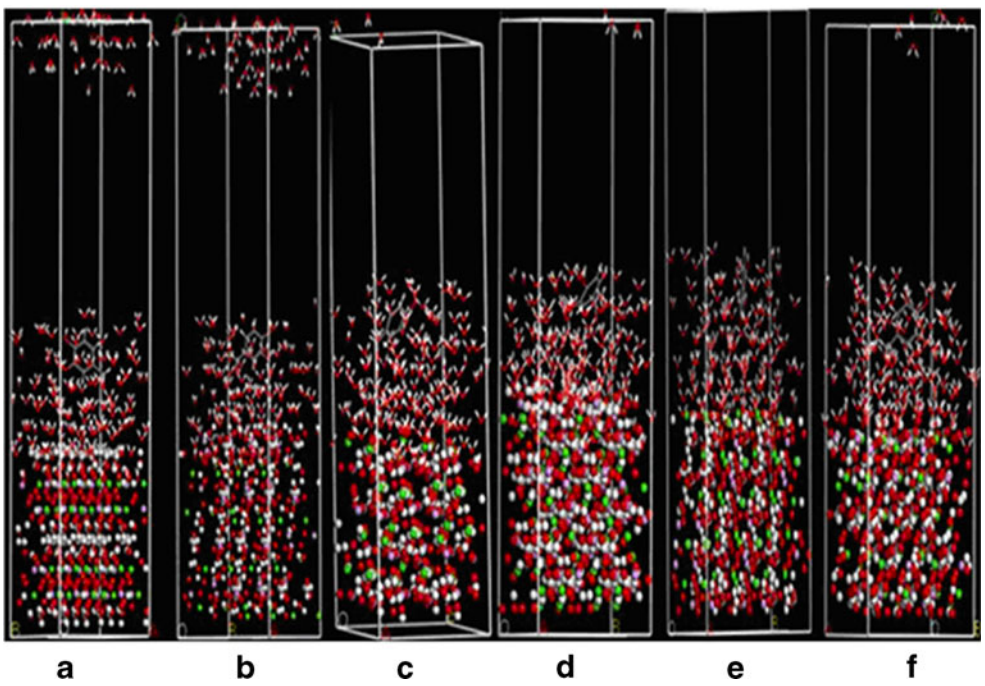

Fig. 3 The final optimized results of Pca adsorption on the different DCPD surfaces: (**a**) (0 2 0), (**b**) (0 2 1), (**c**) (0 4 1), (**d**) (0 6 1), (**e**) ($\bar{2}$ 2 1), (**f**) ($\bar{1}$ 5 1)

Table 2 The adsorption energies of Pca absorption on different DCPD crystal surfaces

Crystal surface	E_{total} (kcal/mol)	E_{Pca} (kcal/mol)	E_{DCPD} (kcal/mol)	E_{H2O} (kcal/mol)	$E_{adsorption}$ (kcal/mol)	$E_{ads\ 2}$ (kcal/mol Å^2)
(0 2 0)	189953.36	32.05	191277.32	5445.34	-6801.35	-26.13
(0 2 1)	190439.94	25.17	190234.47	4827.84	-4647.54	-21.21
(−2 2 1)	203487.06	22.39	203974.69	4541.18	-5058.74	-13.9
(−1 5 1)	200172.33	53.70	198724.46	4496.68	-3102.51	-8.19
(0 4 1)	157189.74	21.84	155643.39	4441.22	-2916.71	-9.11
(0 6 1)	215371.42	27.15	212981.80	4886.48	-2524.01	-5.89

Institute for the Control of Pharmaceutical and Biological Products (NICPBP, Beijing, China), to produce DCPD/Pca precipitation according to Eq. 2. The pH of reaction solution was kept at 7. The amount of adding Pca was determined by hypothesizing a DCPD crystal cell combining with one Pca molecular corresponding to simulation process. DCPD without Pca was synthesized to be used as the control.

$$Ca(NO_3)_2 \cdot 4H_2O + (NH_4)_2HPO_4 = CaHPO_4 \cdot 2H_2O + 2NH_4NO_3 + 2H_2O \quad (2)$$

Characterization

XRD (X'Pert, Philips, Netherlands) was used to analyze the phase components of DCPD/Pca and DCPD. Scans were performed at 40 KV/50 mA using Ni-filtered Cu Kα radiation (λ=0.1542 nm). Data was collected using a stepwise scanning mode with an integration time of 1 s at an interval of 0.02° (2θ).

DCPD/Pca and DCPD powders were mixed with potassium bromide at the mass fraction of 1 wt% then were pressed to get the discs, respectively. The Fourier transform infrared spectroscopy (FTIR) (5700, Nicolet, USA) was used to determine the function groups of DCPD/Pca and DCPD.

Thermal-gravimetric (TG) analysis (STA-449, Netzsch, Germany) were used to determine the Pca content in DCPD. The scanning temperature for TG was from 30°C to 500°C with a heating rate of 10°C / min in air atmosphere. The samples were dried at 80°C for 24 h before test. The weight losses of DCPD powder with and without Pca were determined according to the TG curves. The total weight loss of DCPD powder with Pca including the loss of adsorbed and lattice water and Pca in it whereas the total weight loss of DCPD powder without Pca only including the loss of adsorbed and lattice water in it. Therefore, the content of Pca in DCPD was calculated through Eq. 3.

$$\text{Pca wt\%} = \text{weight loss of DCPD/SMB\%} - \text{weight loss of DCPD\%} \quad (3)$$

Results and discussion

Simulation results

The calculating results of adsorption energies of Pca absorption on different DCPD surfaces are listed in Table 2. It was found that the adsorption energies of the selected crystallographic planes were -26.13 kcal mol^{-1} Å^{-2}, -21.21 kcal mol^{-1} Å^{-2}, -13.9 kcal mol^{-1} Å^{-2}, -8.19 kcal mol^{-1} Å^{-2}, -9.11 kcal mol^{-1} Å^{-2}, -5.89 kcal mol^{-1} Å^{-2}, respectively. The adsorption energies of the system are lower, the system is more stable, and when the Gibbs free energy is less than zero, the reaction is spontaneous from thermodynamics point of view [30, 31]. Among the selected surfaces, the adsorption energy of (0 2 0) crystal surface was the lowest, which indicated that the process of Pca adsorption on the (0 2 0) crystal surface was favorable and spontaneous. Then (0 2 0) crystal surface was selected to further discuss the influence of temperature and binding mode on the adsorption energy. It was also noticeable that

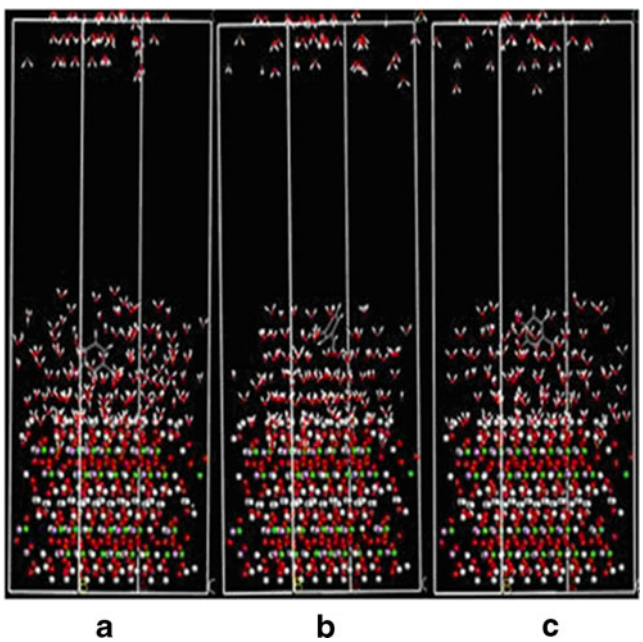

Fig. 4 The models after Pca rotating: (**a**) 45°, (b) 90°, (**c**) 180°

Table 3 The adsorption energies of Pca absorption on DCPD *via* different combinative modes

Angle	E_{total} (kcal/mol)	E_{Pca} (kcal/mol)	E_{DCPD} (kcal/mol)	E_{H2O} (kcal/mol)	$E_{adsorption}$ (kcal/mol)	$E_{ads\ 2}$ (kcal/mol Å^2)
0°	189953.36	32.05	191277.32	5445.34	-6801.35	-26.13
45°	186740.12	43.38	187867.44	4554.59	-5725.29	-22.01
90°	187146.29	37.43	186350.38	4458.27	-3699.79	-14.22
180°	188432.49	40.45	185075.45	4616.06	-1299.47	-4.99

(0 2 0) plane had the most intensive diffraction peak of DCPD according to the XRD testing discussed in the following dissection.

According to the literature, Pca molecule has one aldehyde group and two hydroxyl groups [12]. The influence of different functional groups on the adsorption energy was discussed through rotating the angle (0°, 45°, 90°, 180°) (Fig. 4) of Pca combining with DCPD. In detail, aldehyde group was close to the surfaces when the angle was between 0° and 90°, and hydroxy was close to the surfaces when the angle was between 90° and 180°. The calculating results of the adsorption energy of different combinative modes were listed in Table 3 and the models after rotating were shown in Fig. 4. The present results showed that the unit area adsorption energies ($E\ ads^2$) increased to -4.99 kcal mol^{-1} Å^{-2} when the hydroxyl was next to the crystal surface, and the unit area adsorption energies reduced to -26.13 kcal mol^{-1} Å^{-2} while the aldehyde group was close to the crystal surface. It might be indicated that aldehyde group had the main effect on the adsorption energy, whereas hydroxyl of Pca had no distinct effect.

(0 2 0) crystal surface was selected to calculate the adsorption energy at different temperature (at room temperature 298 K, at body temperature 310 K, and at relatively high-temperature 343 K) to study the influence of different temperature on adsorption energy. The calculating results of adsorption energy at the different temperature were listed in Table 4. It could infer that temperature had no great effects on adsorption energy. Therefore, synthesis DCPD loading with protocatechuic aldehyde at room temperature or at relatively high-temperature had no conspicuous influence on adsorption rate. However, temperature should be kept preferably below 353 K to avoid the phase transformation of DCPD to DCPA [32] and the decomposition of Pca.

Experiment results

The XRD patterns of DCPD/Pca and DCPD were shown in Fig. 5. The diffraction peaks of DCPD/Pca and DCPD were in good agreement with the standard data (JCPDS no: 09-0077) for DCPD (peaks without marker belongs to the DCPA). For DCPD/Pca crystals, the intensity of some of the crystal surface, such as (0 2 0), were more intense than that of the control DCPD, which resulted from the preferential growth of (0 2 0) crystal surface [28]. In general, growth of calcium phosphate was depended on pH, temperature, Ca/P ratio, and the presence of ions or biomolecular [33]. DCPD formation from solution was favored at the lower pH [33]. Pca is the acidic component based on its molecular structure information. Pca might act as the promoter for preferential growth of DCPD due to its acidic group. In addition, a new peak owing to crystal surface (1 1 0) was also presented in the DCPD/Pca, which might be due to the special structure of the monoclinic system of DCPD: crystal lattice, a, is approximately equal to c, which might result in (0 1 1) and (1 1 0) alternative appearance.

Eight kinds of representative peaks were selected, and the change of their 2θ and plane spacing (d) and the detail deviation of various 2θ and d were listed in Table 5. Compared with the control DCPD, all the deviation were in the normal error scope [34], which indicated that the adsorption of Pca on (0 2 0) crystal surface has no influence on the crystal structure of DCPD. Moreover, the peak width has no change, which showed that loaded with Pca has no influence on the crystallinity and grain size of DCPD.

The infrared spectra of the DCPD/Pca and DCPD were presented in Fig. 6, which have similar patterns. However, the peaks at 1295 cm^{-1} in the spectrum of DCPD/Pca might be attributed to the characteristic peak of Pca molecular [28,

Table 4 The adsorption energy of Pca absorption on DCPD at different temperatures

T	E_{total} (kcal/mol)	E_{Pca} (kcal/mol)	E_{DCPD} (kcal/mol)	E_{H2O} (kcal/mol)	$E_{adsorption}$ (kcal/mol)	$E_{ads\ 2}$ (kcal/mol Å^2)
298 K	189953.36	32.05	191277.32	5445.34	-6801.35	-26.13
310 k	189994.56	47.40	191269.39	5384.95	-6707.18	-25.78
343 k	189803.55	64.12	191076.78	5289.18	-6626.53	-25.47

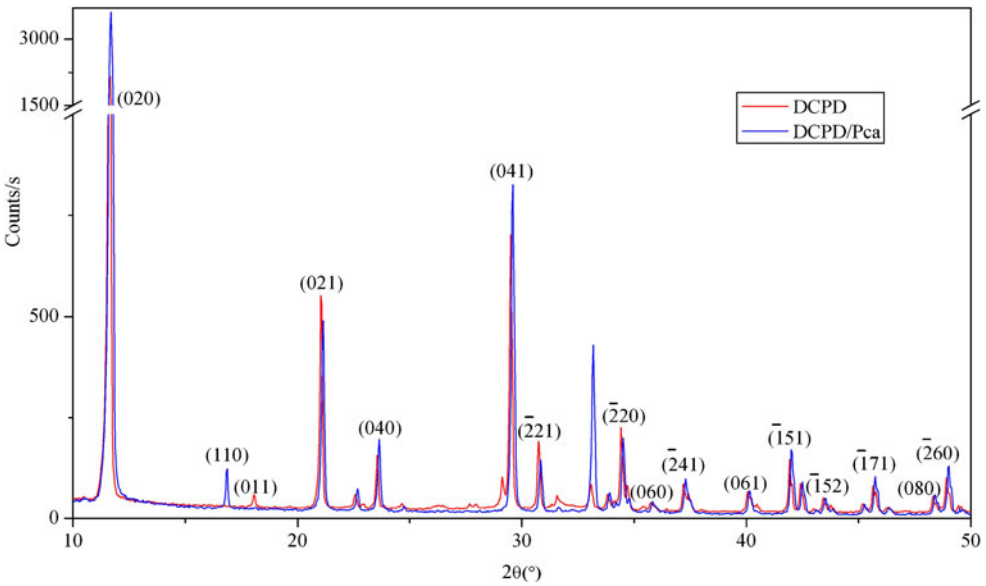

Fig. 5 XRD patterns of the DCPD and DCPD/Pca

Table 5 The changes of the 2θ and plane spacing (d) for the selected peaks. deviation$_1$=|θ_2-θ_1|/θ_1; deviation $_2$=|d_2-d_1|/d_1

Crystal surface		(0 2 0)	(0 2 1)	(0 4 1)	(−2 2 1)	(−2 2 0)	(−2 0 2)	(1 5 1)	(2 4 1)
DCPD	$2\theta_1$(°)	11.628	20.928	29.271	30.500	34.127	34.410	41.521	50.176
	d $_1$(Å)	7.610	4.245	3.051	2.931	2.627	2.606	2.175	1.818
DCPD/Pca	$2\theta_2$(°)	11.675	21.009	29.353	30.580	34.205	34.473	41.600	50.259
	d $_2$(Å)	7.580	4.229	3.043	2.923	2.622	2.600	2.171	1.815
	deviation$_1$	0.398%	0.389%	0.280%	0.262%	0.228%	0.183%	0.190%	0.165%
	deviation$_2$	0.394%	0.377%	0.262%	0.273%	0.190%	0.230%	0.184%	0.165%

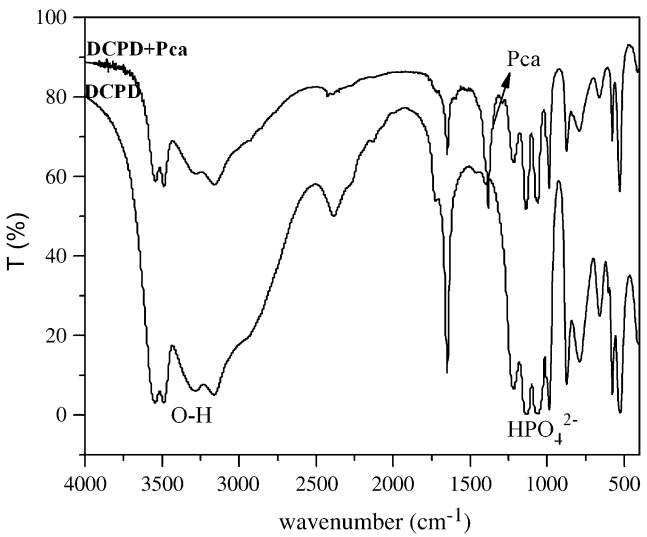

Fig. 6 FTIR Spectra of DCPD and DCPD/Pca

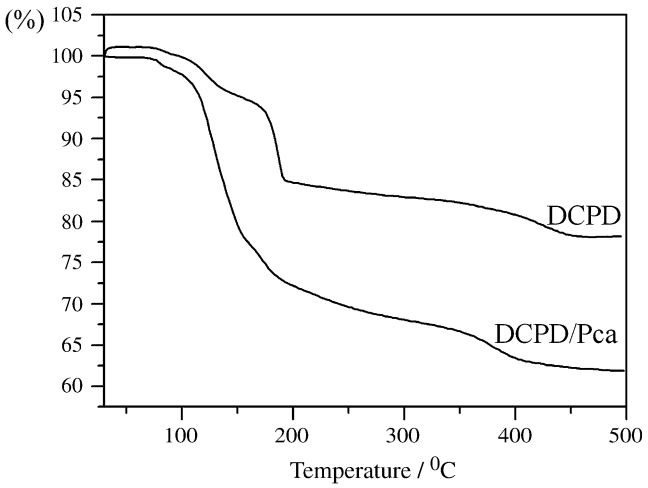

Fig. 7 TG curves of DCPD and DCPD/Pca

35]. They have a broad envelope between 2000 and 3900 cm^{-1}, which include the O–H stretch of HPO_4^{2-}, water and $v_1(a_1)$ vibrations of the former [28]. The peak owing to $v_2(a_1)$ vibration of HPO_4^{2-} occurs at 985 cm^{-1}, $v_3(a_1)$ at 872 cm^{-1}, $v_4(a_1)$ at 526 cm^{-1}, $v_5(a_1)$ at 1217 cm^{-1} and $v_6(e)$ at 1062 cm^{-1} [35].

Figure 7 illustrated the TG curves for the synthesized powders in the temperature range of 30–500 °C. Based on the TG curve of DCPD and DCPD/Pca, it can be calculated that total weight losses of Pca was 16 wt%, compared with the total amount of Pca (20 wt %) we added. There was 4 wt % deviation of total amount, which might be because some of the Pca molecular did not adsorb on DCPD crystal surface.

Conclusions

Based on software simulation, it was concluded that Protocatechuic aldehyde mostly absorbed on the (0 2 0) crystal surface of DCPD, and the aldehyde group was the main influencing factor other than hydroxyl, and temperature has no distinct effects on the adsorption energy. Moreover, the present XRD and eight kinds of representative peaks results confirmed that Pca induced the preferential growth of (0 2 0) crystal surface in DCPC/Pca whereas it had no influence on the crystal structure, the crystallinity and grain size of DCPD. FTIR and TG results showed that the characteristic peak of Pca was at 1295 cm^{-1} and the content of Pca in DCPD was 16%, respectively.

Acknowledgments The present study was supported by National Natural Science Foundation of China (30470484) and Program for New Century Excellent Talents in University (NCET-05-0797), Ministry of Education, China.

References

1. Brown WE, Chow LC (1983) A new calcium phosphate setting cement. J Dent Res 62:672
2. Bohner M (2000) Calcium orthophosphates in medicine: from ceramics to calcium phosphate cements. Injury 31:37–47
3. Amit KJ, Ramesh P (2000) Skeletal drug delivery system. Int J Pharm 206:1–12. doi:10.1016/S0378-5173(00)00468-3
4. Ginebra MP, Traykova T, Planell JA (2006) Calcium phosphate cements as bone drug delivery system: A review. J Control Release 113:102–110. doi:10.1016/j.jconrel.2006.04.007
5. Elliott JC (1994) General chemistry of the calcium orthophosphate. In: Elliott JC (ed) Structure and chemistry of the apatites and other calcium orthophosphate. Elsevier, London, pp 23–30
6. Constantz BR, Barr BM, Ison IC, Fulmer MT, Baker J, Mckinney L, Goodman SB, Gunasekaren S, Delaney DC, Ross J, Poster RD (1998) Histological, chemical, and crystallographic analysis of four calcium phosphate cements in different rabbit osseous sites. J Biomed Mater Res 43:451–461. doi:10.1002/(SICI)1097-4636(199824)43:4<451::AID-JBM13>3.0.CO;2-Q
7. Munting E, Mirtchi A, Lemaitre J (1993) Bone repair of defects filled with a phosphocalcic hydraulic cement: an in vivo study. J Mater Sci Mater Med 4:337–344. doi:10.1007/BF00122290
8. Wong RWK, Rabie ABM (2006) Traditional Chinese medicines and bone formation-A review. J Oral Maxillofac Surg 64:828–837. doi:10.1016/j.joms.2006.01.017
9. Hu P, Liang QL, Luo GA, Zhao ZZ, Jiang ZH (2005) Multi-component HPLC fingerprinting of Radix Salviae Miltiorrhizae and its LC-MS-MS identification. Chem Pharm Bull 53:677–683. doi:10.1248/cpb.53.677
10. Chae HJ, Chae SW, Yun DH, Keum KS, Yoo SK, Kim HR (2004) Prevention of bone loss in ovariectomized rats: the effect of Salvia miltiorrhiza extracts. Immunopharm Immunot 26:35–144. doi:10.1081/IPH-120029951
11. Ding Y, Soma S, Takano YT, Matsumoto S, Sakuda M (1995) Effects of salvia miltiorrhiza bunge (SMB) on MC3T3–E1 cells. J Osaka Univ Dent Sch 35:21–27
12. Liu YR, Qu SX, Maitz MF, Tan R, Weng J (2007) The effect of the major components of Salvia Miltiorrhiza Bunge on bone marrow cells. J Ethnopharmacol 111:573–583. doi:10.1016/j.jep.2007.01.005
13. Qu SX, Weng J, Feng B, Jiang CX, Jiang CZ, Wang J (2005) Preliminary study of calcium phosphate immobilized with Chinese medicine. J Mater Sci 40:3035–3037. doi:10.1007/s10853-005-2397-6
14. Lin FH, Dong GC, Chen KS, Jiang GJ, Huang CW, Sun JS (2003) Immobilization of Chinese herbal medicine onto the surface-modified calcium hydrogenphosphate. Biomaterials 24:2413–2422. doi:10.1016/S0142-9612(03)00031-0
15. Sun JS, Dong GC, Lin CY, Sheu SY, Lin FH, Chen LT, Chang WHS, Wang YJ (2003) The effect of Gu-Sui-Bu (Drynaria fortunei J. Sm) immobilized modified calcium hydrogenphosphate on bone cell activities. Biomaterials 24:873–882. doi:10.1016/S0142-9612(02)00372-1
16. Yao CH, Tsai HM, Chen YS, Liu BS (2005) Fabrication and evaluation of a new composite composed of tricalcium phosphate, gelatin, and chinese medicine as a bone substittute. J Biomed Mater Res B 75:277–288
17. Qu SX, Weng J, Feng B, Li MH, Huang C, Liu YR, Xie HD (2005) Investigation of calcium phosphate cement containing chinese medicine proceeding of international symposium on quality of bone and scaffold. Biomaterials :156–160
18. Yu XH, Qu SX, Liu YR, Shen R, Li XH, Zhao W, Weng J (2006) Investigation on the in vitro degradation and release behaviors of calcium phosphate containing Chinese medicine. Key Eng Mater 284-286. doi:10.4028/www.scientific.net/KEM.284-286.395
19. Wang XJ, Selvam P, Lv C, Kubo M, Miyamoto A (2004) A theoretical study on the cyclopropane adsorption onto the copper surfaces by density functional theory and quantum chemical molecular dynamics methods. J Mol Catal A: Chem 12:189–198. doi:10.1016/j.molcata.2004.04.044
20. Dubey DK, Tomar V (2008) Microstructure dependent dynamic fracture analyses of trabecular bone based on nascent bone atomistic simulations. Mech Res Commun 35:24–31. doi:10.1016/j.mechrescom.2007.10.011
21. Zhou HL, Wu T, Dong XL, Wang Q, Shen JW (2007) Adsorption mechanism of BMP-7 on hydroxyapatite (0 01) surfaces. Biochem Biophys Res Commun 361:91–96. doi:10.1016/j.bbrc.2007.06.169
22. Shen JW, Wu T, Wang Q, Pan HH (2008) Molecular simulation of protein adsorption and desorption on hydroxyapatite surfaces. Biomaterials 29:513–532. doi:10.1016/j.biomaterials.2007.10.016
23. Bhowmik R, Katti KS, Katti D (2007) Molecular dynamics simulation of hydroxyapatite – polyacrylic acid interfaces. Polymer 48:664–674. doi:10.1016/j.polymer.2006.11.015
24. Bhowmik R, Katti KS, Verma D, Katti DRC (2007) Probing molecular interactions in bone biomaterials: Through molecular

dynamics and Fourier transform infrared spectroscopy. Mater Sci Eng 27:352–371. doi:10.1016/j.msec.2006.05.048
25. Accelry (2002) Materials studio 4.0 discover (San Diego CA)
26. Curry NA, Jones DW (1971) Crystal structure of brushite, calcium hydrogen orthophosphate dihydrate: a neutron-diffraction investigation. J Chem Soc A:3725–3729. doi:10.1039/J19710003725
27. Heijnen WMM, Hartman P (1991) Structure morphology of gypsum ($CaSO4{\cdot}2H_2O$), brushite ($CaHPO_4{\cdot}2H_2O$) and pharmacolite ($CaHAsO_4{\cdot}2\ H_2O$). J Cryst Growth 108:290–300
28. Anee TK, Meenakshi SN, Arivuolic D, Ramasamy P, Narayana KS (2005) Influence of an organic and an inorganic additive on the crystallization of dicalcium phosphate dehydrate. J Cryst Growth 285:380–387. doi:10.1016/j.jcrysgro.2005.08.036
29. Yin KL, Zou DH, Zhong J, Xu DJ (2007) A new method for calculation of elastic properties of anisotropic material by constant pressure molecular dynamics. Comp Mater Sci 38:538–542. doi:10.1016/j.commatsci.2005.10.008
30. Ren H, Zhang QY, Chen XW, ZhaoW ZJP, Zhang HP, Zeng R, Xu S (2007) A molecular simulation study of a series of cyclohexanone formaldehyde resins: Properties and applications in plastic printing. Polymer 48:887–893. doi:10.1016/j.polymer.2006.12.016
31. Zhao W, Zhang QY, Chen T, Zhang JP, Lu TL, Zhang H (2009) Molecular dynamic simulation of adsorption of polyelectrolyte on the polystyrene microspheres. J Mater Sci Eng 27:329–331. doi:cnki:sun:clkx.0.2009-03-002
32. Elliott JC (1994) General chemistry of the calcium orthophosphates. In: Elliott JC (ed) Structure and chemistry of the apatites and other calcium orthophosphate. Elsevier, London, pp 31–35
33. LeGeros RZ (1991) Formation of calcium phosphates in vitro. In: Myers HM (ed) Calcium phosphates in oral biology and medicine. Karger, New York, pp 46–66
34. Liu EH, Liu PA (2003) The analysis of principle and application for x-ray diffraction. Benjing
35. Anee TK, Palanichamy M, Ashok M, Meenakshi SN, Narayana KS (2004) Influence of iron and temperature on the crystallization of calcium phosphates at the physiological pH. Mater Lett 58:478–482. doi:10.1016/S0167-577X(03)00529-9